Evaluating Retinal Function in Age-Related Maculopathy with the ERG Photostress Test

Alison M. Binns and Tom H. Margrain

PURPOSE. To evaluate the diagnostic potential of the electroretinogram (ERG) photostress test and the focal cone ERG in age-related maculopathy (ARM).

METHODS. The cohort comprised 31 patients with ARM and 27 age-matched control subjects. The ERG photostress test was used to monitor cone adaptation after intense light adaptation. Focal 41- and 5-Hz cone ERGs were recorded monocularly (central 20°) to assess steady state retinal function. Univariate analysis identified electrophysiological parameters that differed between groups, and receiver operating characteristic (ROC) curves were constructed to assess their diagnostic potential. Logistic regression analysis determined the diagnostic potential of a model incorporating several independent predictors of ARM.

RESULTS. The rate of recovery of the ERG photostress test was reduced (recovery was slower) in subjects with ARM. The parameter exhibited good diagnostic potential ($P = 0.002$, area under ROC curve $= 0.74$). The implicit times of the 5-Hz (a-wave, $P = 0.002$; b-wave, $P < 0.001$) and the 41-Hz ($P < 0.001$) focal cone ERGs were increased, and the 41-Hz focal cone ERG amplitude ($P = 0.003$) and focal to full-field amplitude ratio ($P = 0.001$) were reduced in the ARM group. Logistic regression analysis identified three independent predictors of ARM, including the rate of recovery of the ERG photostress test.

CONCLUSIONS. Early ARM has a marked effect on the kinetics of cone adaptation. The clinical application of the ERG photostress test increases the sensitivity and specificity of a model for the diagnosis of ARM. Improved assessment of the functional integrity of the central retina will facilitate early diagnosis and evaluation of therapeutic interventions. (*Invest Ophthalmol Vis Sci.* 2007;48:2806–2813) DOI:10.1167/iovs.06-0392

Age-related macular degeneration (AMD) is a condition that affects the photoreceptors, retinal pigment epithelium (RPE), Bruch's membrane, and choriocapillaris. It is the principal cause of blindness in the developed world and currently affects approximately 12.7 million people in Europe and North America.[1,2] Age-related maculopathy (ARM) is a term applied to the early stages of the AMD disease process, in which visual acuity is often normal.[3]

Given the substantial social and economic impact of the disease, it is not surprising that there is a considerable research effort to develop therapeutic interventions (e.g., photodynamic therapy,[4] transpupillary thermotherapy,[5] radiation therapy[6] pharmacologic therapy,[7] and surgical intervention[8]). Sensitive measures of retinal function are an essential requirement to assess the efficacy of these interventions and for the early identification of at-risk individuals.

Electrodiagnostic tests are capable of evaluating subtle abnormalities in central retinal function and have a role in the assessment of ARM and AMD. Previous studies have shown that ARM and AMD are associated with a reduction in response amplitude and an increase in latency of the steady state focal cone ERG and the multifocal cone ERG,[9–16] which is consistent with histologic and psychophysical evidence of cone loss.[17–20] Anatomic and psychophysical evidence suggests that parafoveal rods are also affected in ARM,[17–19] and these findings are supported by the presence of prolonged response latencies[21] and reduced amplitudes[22] in the multifocal rod ERG.

Procedures that evaluate the kinetics of cone and rod adaptation, may be even more sensitive to ARM than are steady state measures of visual function.[23,24] However, obtaining objective electrophysiological measures of the kinetics of rod adaptation is technically challenging. For example, although central rods are affected in ARM[18,25,26] their lack of directional sensitivity makes the recording of focal rod responses problematic.[27] An additional difficulty in the clinic is that rod dark adaptation is a slow process.

Conversely, the kinetics of cone adaptation are relatively fast. The visual evoked potential (VEP) has been used to obtain an objective measure of cone adaptation.[28,29] However, the VEP reflects the activity of the entire visual pathway, and postretinal disease delays its recovery,[29] limiting the value of this measure in outer retinal diseases such as ARM. The ERG photostress test monitors the recovery of the focal 41-Hz ERG after a period of intense light adaptation.[30] The first harmonic of the 41-Hz flicker ERG is dominated by bipolar cell activity,[31–34] and so provides a more direct measure of outer retinal function than does the VEP. The recovery of the 41-Hz ERG is primarily dependent on photopigment regeneration,[30] and hence the ERG photostress test may have an important role in the evaluation of ARM and AMD.

The purpose of this study was to assess the efficacy of the ERG photostress test at detecting early functional changes in ARM, compared with ERG measures of steady state cone function. In this report, we will demonstrate that the rate of recovery of the ERG photostress test provides good discrimination between participants with ARM and age-matched control subjects, and is a significant parameter in a multivariate diagnostic model. This finding could facilitate the earlier diagnosis of ARM and improve the sensitivity of the assessment of changes in retinal function after treatment.

MATERIALS AND METHODS

Participants

The cohort comprised 31 patients with ARM, recruited from the Eye Unit at the University Hospital of Wales, Cardiff. The inclusion criteria were: age at least 55 years, a corrected VA of 0.5 logMAR (logarithm of the minimum angle of resolution), or better in the test eye, and a diagnosis of ARM according to the International Classification and Grading System,[3] with no coexisting ocular–fundal abnormality. A diagnosis of ARM required the presence of one or more of the follow-

ing macular signs: drusen and focal hyperpigmentation or hypopigmentation, in the absence of geographic atrophy or exudative AMD. The presence of small (<63 μm), hard drusen alone within the macular area was not considered to be diagnostic of ARM. Diagnosis was based on the appearance of 30° diameter stereo fundus images (3-DX Stereo Disc Camera; Nidek Co. Ltd., Gamagori, Japan), which were obtained through dilated pupils on the day that the ERGs were recorded. Representative fundus photographs of the test eye of eight participants with ARM are shown in Figure 1, along with the corresponding visual acuities.

The control group consisted of 27 individuals recruited from the Eye Clinic at Cardiff University, all of whom had a corrected visual acuity of logMAR 0.2 or better and a normal retinal and optic nerve head appearance in both eyes.

Potential recruits to either group were excluded from the study if they had a history of systemic disease (or medication) likely to affect retinal function, a history of photosensitive epilepsy, or media opacities detrimental to the acquisition of clear fundus images. The clinical characteristics of the groups are described in Table 1. In all cases, the eye chosen for ERG recording was the eye with ARM or, in the case of bilateral ARM and control subjects, the eye with the better visual acuity.

The study adhered to the Tenets of the Declaration of Helsinki and was approved by the South East Wales Research Ethics Committee. Written, informed consent was obtained from all participants before participation in the study.

ERG Recording

Pupils were dilated with 1 drop of 1.0% tropicamide before ERG recording. Silver-silver chloride, 9-mm diameter, touchproof skin electrodes (Viasys Healthcare Ltd., Warwick, UK) were applied to the midfrontal and outer canthus positions, acting as ground and reference electrodes, respectively. Skin electrodes were attached using surgical tape (Blenderm; 3M, St. Paul, MN) after preparing the skin with gel (Nuprep; D. O. Weaver & Co., Aurora, CO), and filling electrode cups with electrolyte electrode gel (Teca, Pleasantville, NY). A DTL fiber active electrode[35] (Unimed Electrode Supplies, Surrey, UK) was positioned in the lower fornix of the test eye. All ERGs were recorded without local anesthetic or methylcellulose solution.

An evoked potential monitoring system (Medelec Synergy EP; Oxford Instruments Medical, Surrey, UK) was used to record all ERGs. All responses were band-pass filtered from 1 to 100 Hz and digitally averaged. One hundred sweeps were averaged per trace. An artifact-reject setting allowed the exclusion of traces contaminated by blinks or eye movements.

Stimuli were generated with a miniature Ganzfeld LED stimulator. The head stage of the stimulator comprised an array of amber LEDs (peak λ = 595 nm, half-height bandwidth = 17 nm) set behind a circular diffuser. All stimuli had an average luminance of 30 phot cd · m^{-2} (3.18 log phot Td, assuming a pupil diameter of 8 mm, and making no correction for the Stiles-Crawford effect). The stimulus subtended 20° at the eye, viewed from a distance of 14 cm and was set within a luminance-matched Ganzfeld surround to suppress responses from the peripheral retina. All luminances were measured with a light meter (LS-110; Konica Minolta, Osaka, Japan). Conversion from photopic to scotopic luminances was calculated according to data supplied by Wyszeki and Stiles.[36] Since this conversion factor is only strictly applicable to monochromatic light sources, an approximation of scotopic luminance was obtained by using the wavelength of peak LED transmission in all calculations.

Flicker ERGs were recorded in response to a square-wave stimulus presented at a temporal frequency of 41 Hz (flash duration 12 ms). Transient responses were also obtained, using a square-wave, 5-Hz stimulus (flash duration, 100 ms). A 50-ms time base was used for recording the 41-Hz ERG, and a 200 ms time base was used for recording the 5-Hz ERG. Examination of the energy spectrum of the focal 5-Hz ERG indicates that the components that comprise the a- and b-waves of the response are at frequencies lower than 45 Hz. Higher-
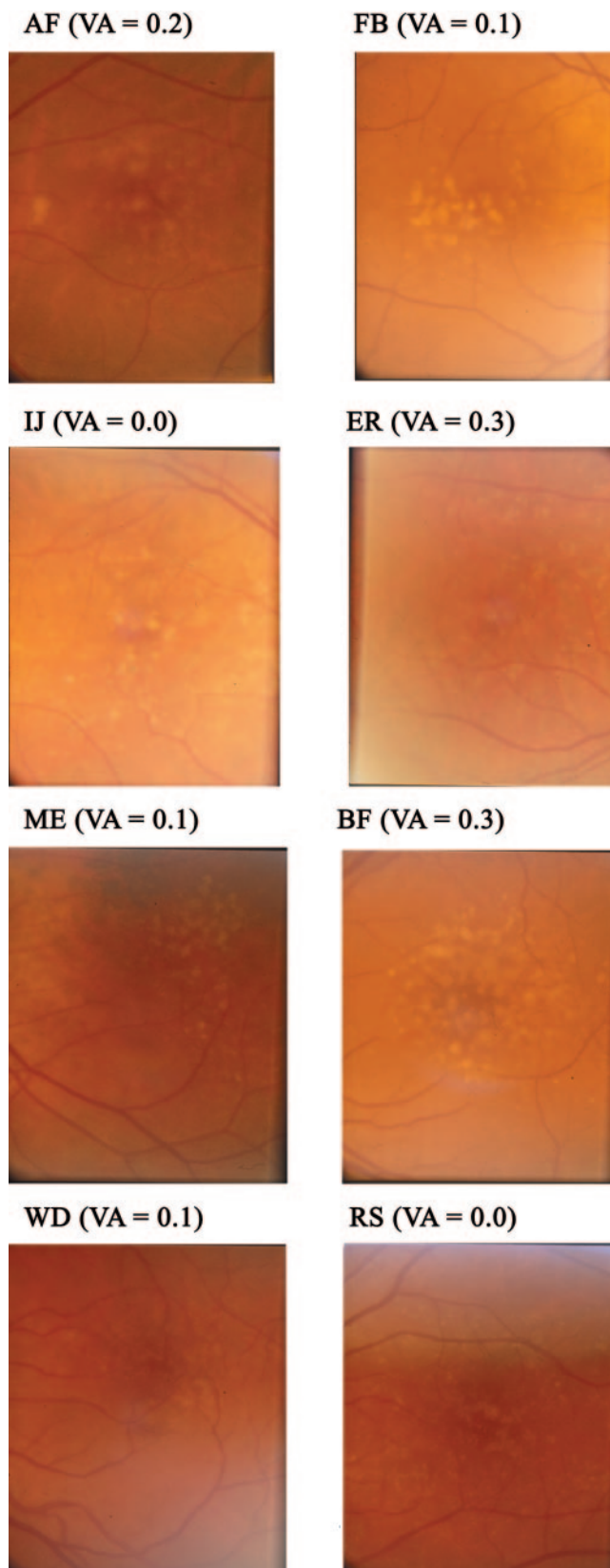

FIGURE 1. Photographs of the fundus appearance of eight typical participants with ARM, along with their logMAR visual acuities.

frequency signals may be attributed to oscillatory potentials and extraneous noise. Therefore, the signal-to-noise ratio of the a- and b-wave components of the ERG was improved by using Fourier analysis to

TABLE 1. Summary of Characteristics of Participant Groups

	Control (*n* = 27)	ARM (*n* = 31)	Univariate Comparison of Groups
Age, mean years (SD)	71.7 (7.0)	72.4 (8.0)	*P* = 0.71
Gender (% female)	46	52	*P* = 0.72
Acuity of test eye, mean logMAR (SD)	0.04 (0.07)	0.20 (0.15)	*P* < .001
Diagnosis of ARM in test eye	0	31	
Diagnosis in fellow eye			
ARM	0	12	
Geographic atrophy	0	8	
Exudative AMD	0	11	

There was no significant difference in age or gender balance between the control and ARM groups. Visual acuity was significantly worse in the ARM group than in the control group.

remove frequencies higher than 45 Hz. Fourier analysis was implemented in commercial software (Excel 2003; Microsoft. Redmond, WA). First, the average ERG signal obtained during the first 6 ms was set to 0 V, and baseline drift was corrected by subtracting a ramp function such that the final 20 ms of the trace also had an average amplitude of 0 V. Subsequently, the Fourier coefficients for the first nine harmonics were determined, and these were used to reconstruct the signal. In this way, frequencies above 45 Hz (the ninth harmonic) were removed from the signal. The measurement of implicit times and amplitudes of the a- and b-waves was objectified by measuring the minima and maxima within a specified time window of 15 to 30 ms (a-wave) and 35 to 50 ms (b-wave). The amplitude and time-to-peak of the first harmonic of the focal 41-Hz ERG were also determined by using Fourier analysis.

Full-field ERG responses were also recorded for the same stimuli (30 phot cd · m^{-2}, temporal frequency 5 and 41 Hz). This allowed the determination of a focal-to-full-field amplitude ratio.

The amber stimulus of 30 phot cd · m^{-2} (1.44 scot cd · m^{-2}) used to record all focal cone responses had an average illuminance of 1.86 log scot Td (assuming an 8-mm pupil). Thus, the 5-Hz ERG may have included a small rod contribution, as the rods do not saturate until 3.30 log scot Td.[37] A control study, however, suggested that any rod contribution was minimal. This study recorded both the 41- and 5-Hz focal cone ERGs from a healthy normal subject (AMB), and then again with the same stimuli presented on a rod-saturating blue background which raised the scotopic illuminance to 3.30 log scot Td. The adapting background had the potential to desensitize the rods and the cones; but, since rods do not contribute to ERGs recorded with stimuli of high temporal frequencies,[38] any reduction in amplitude of the 41-Hz ERG when the background was added must have been due to desensitization of the cones alone. If the rods were contributing to the 5-Hz focal

cone ERG, it was hypothesized that the transient response would be reduced in amplitude to a greater extent than would the flicker response by the introduction of the background. The 5- and 41-Hz ERGs were reduced by a comparable amount (24% and 32%, respectively), suggesting that the rod contribution to the 5-Hz ERG was minimal.

Recording of the ERG Photostress Test

The ERG photostress test involved the recording of a baseline 41-Hz focal cone ERG (the average of 200 sweeps) to determine the prebleach response amplitude. The eye was subsequently light-adapted to a bright white background (5.6 log phot Td) for a period of 2 minutes. Because of the Stiles-Crawford effect, not all light reaching the retina through the dilated pupil is effectively absorbed by the directionally sensitive cones. The effective retinal illuminance was calculated as 5.3 phot Td, which bleached approximately 86% of the cone visual pigment.[39] The bleaching light, which had a central fixation cross, subtended 40° at the eye and was presented within the Ganzfeld bowl, immediately below the flickering amber stimulus. After cessation of the bleaching, the participant redirected his or her gaze to the flickering stimulus, and 100 sweeps were averaged every 20 seconds for 5 minutes. This procedure allowed approximately 10 seconds for the participant to relax between each recording period.

Fourier analysis was used to determine the phase and amplitude of the first harmonic of the prebleach 41-Hz ERG. The amplitude of postbleach ERG signals was also determined with Fourier analysis, but the phase was locked to match that of the prebleach signal. Each participant's amplitude recovery data was then modeled, on a least-squares fit basis, by using a first-order exponential function in the form:

$$a(t) = a_0[1 - B \exp(-t/\tau)], \qquad (1)$$

Control Subjects (A)   **Subjects with ARM (B)**

20 µV

100 ms

FIGURE 2. Superimposed raw 5-Hz focal cone ERGs of all control subjects (**A**), and the individual traces of all participants with ARM (**B**). Most, but not all, participants were shown to have clear a- and b-waves, but there was marked between-participant variability in response amplitude.

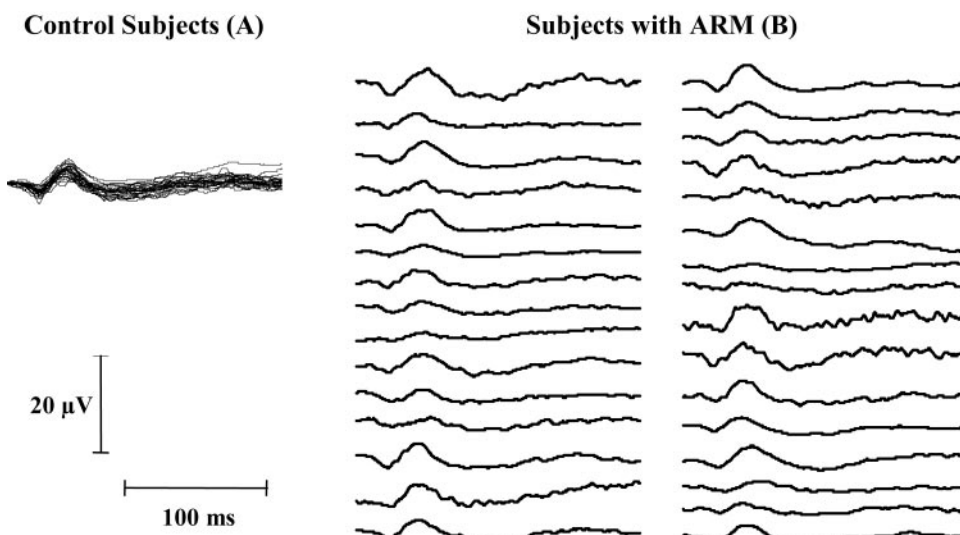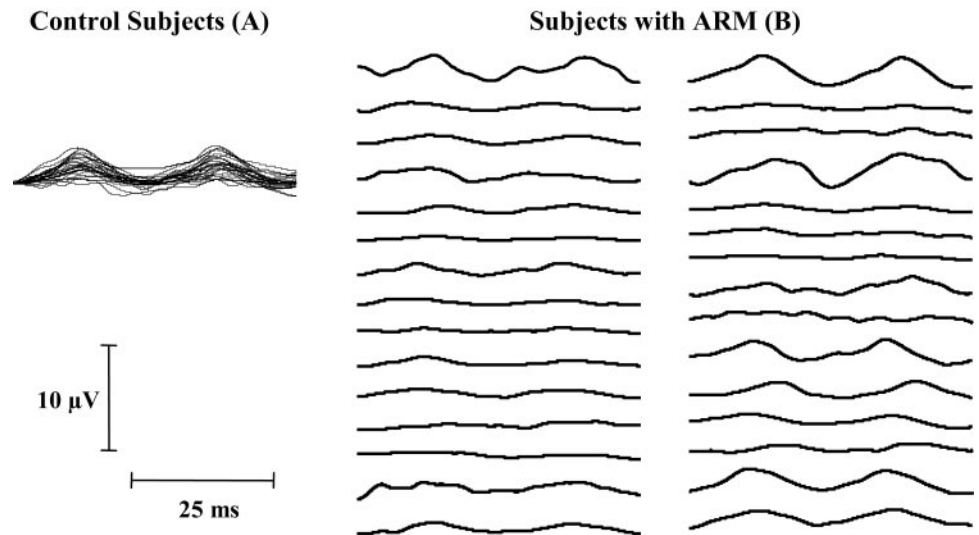**Control Subjects (A)**   **Subjects with ARM (B)**

FIGURE 3. Superimposed raw 41-Hz focal cone ERGs of all control subjects (**A**) and the individual traces of all participants with ARM (**B**). Two clear response peaks were shown in most, but not all, participants. There was marked between-participant variability in response amplitude.

where $a(t)$ is the amplitude of the ERG, a_o is the unbleached amplitude, B is the initial bleaching, τ is the time constant of recovery, and t is the time after bleaching. Assuming that the final, recovered amplitude of the first harmonic would be approximately the same as the prebleach value, two prebleach values were plotted on the curves at a very late time, 24 hours after bleaching, where recovery was assumed to be complete. When fitting the model, B was constrained to be within the range of 0 to 1, and a_o and τ were free parameters of the fit. The parameter assessed for all participants was the time constant of recovery (τ). This constant was converted to a rate-of-recovery parameter ($1/\tau$, min^{-1}). A smaller value for $1/\tau$ indicated a slower rate of recovery.

Analysis

The distribution of the data for each of the electrophysiological parameters was tested for normality by using the Shapiro-Wilkes W test. The ability of each individual parameter to distinguish between the subjects with ARM and the normal control subjects was determined by using an unpaired *t*-test for normally distributed data or, in the case of data that were not normally distributed, the Mann-Whitney test. $P < 0.05$ was taken as representing a significant difference. Individual receiver operating characteristic (ROC) curves were constructed for those parameters that showed a significant difference between the ARM and normal control groups, and the area under the curve was calculated.

To identify independent predictors of ARM and to exploit the full diagnostic potential of the test battery, a logistic regression analysis was undertaken, in which electrophysiological parameters were used as continuous explanatory variables. To avoid including all the variables and run the risk of overfitting the logistic regression model, only those parameters that yielded a statistically significant difference between the two groups in the univariate analysis were included in the logistic regression analysis. Initially, each variable in the regression model was considered individually before running a backward stepwise analysis based on the method of maximum likelihood estimation. Explanatory variables were removed from the model if their significance exceeded $P < 0.1$. The goodness of fit of the regression model was evaluated by plotting an ROC curve and determining the area under the curve. All statistical analysis was undertaken with commercial software (SPSS ver. 12; SPSS, Chicago, IL).

RESULTS

The raw transient (5 Hz) and steady state (41 Hz) focal cone ERG responses from all control subjects and participants with ARM are shown in Figures 2 and 3, respectively. The between-participant variability in the amplitude of the responses is apparent, within both the control and ARM groups. To reduce

TABLE 2. Mean Amplitudes and Implicit Times of the 5- and 41-Hz Focal Cone ERGs, Mean Time Constants of Recovery for the ERG Photostress Test, and the Statistical Significance of the Univariate Analysis between the Group with ARM and the Normal Control Group for Each Parameter

	Control	ARM	Univariate Comparison of Groups	Area under ROC Curve
5-Hz ERG				
a-Wave implicit time (ms)	22.50 (0.29)	24.07 ($\pm$0.31)	$P = 0.002$	0.74
a-Wave amplitude (μV)	1.52 ($\pm$0.14)	1.30 (0.11)	$P = 0.21$	
b-Wave implicit time (ms)	42.66 (0.33)	45.37 (0.49)	$P < 0.001$	0.77
b-Wave amplitude (μv)	3.96 (0.28)	3.42 (0.24)	$P = 0.15$	
Focal: full-field a-wave amplitude	0.1078 (0.0096)	0.0907 (0.0071)	$P = 0.15$	
Focal: full-field b-wave amplitude	0.1342 (0.0065)	0.1177 (0.0080)	$P = 0.12$	
41-Hz ERG				
Implicit time (ms)	11.60 (0.20)	13.21 (0.38)	$P < 0.001$	0.73
Amplitude (μV)	1.98 (0.17)	1.28 (0.16)	$P = 0.003$	0.73
Focal: full-field amplitude	0.153 (0.013)	0.101 (0.010)	$P = 0.001$	0.74
Dynamic Focal Cone ERG				
Rate of recovery ($1/\tau$ min^{-1})	0.372 (0.074)	0.183 (0.048)	$P = 0.002$	0.74

The area under the ROC curve is also given for all parameters that differ significantly between groups on univariate analysis. The values in parentheses denote the SE of the mean.
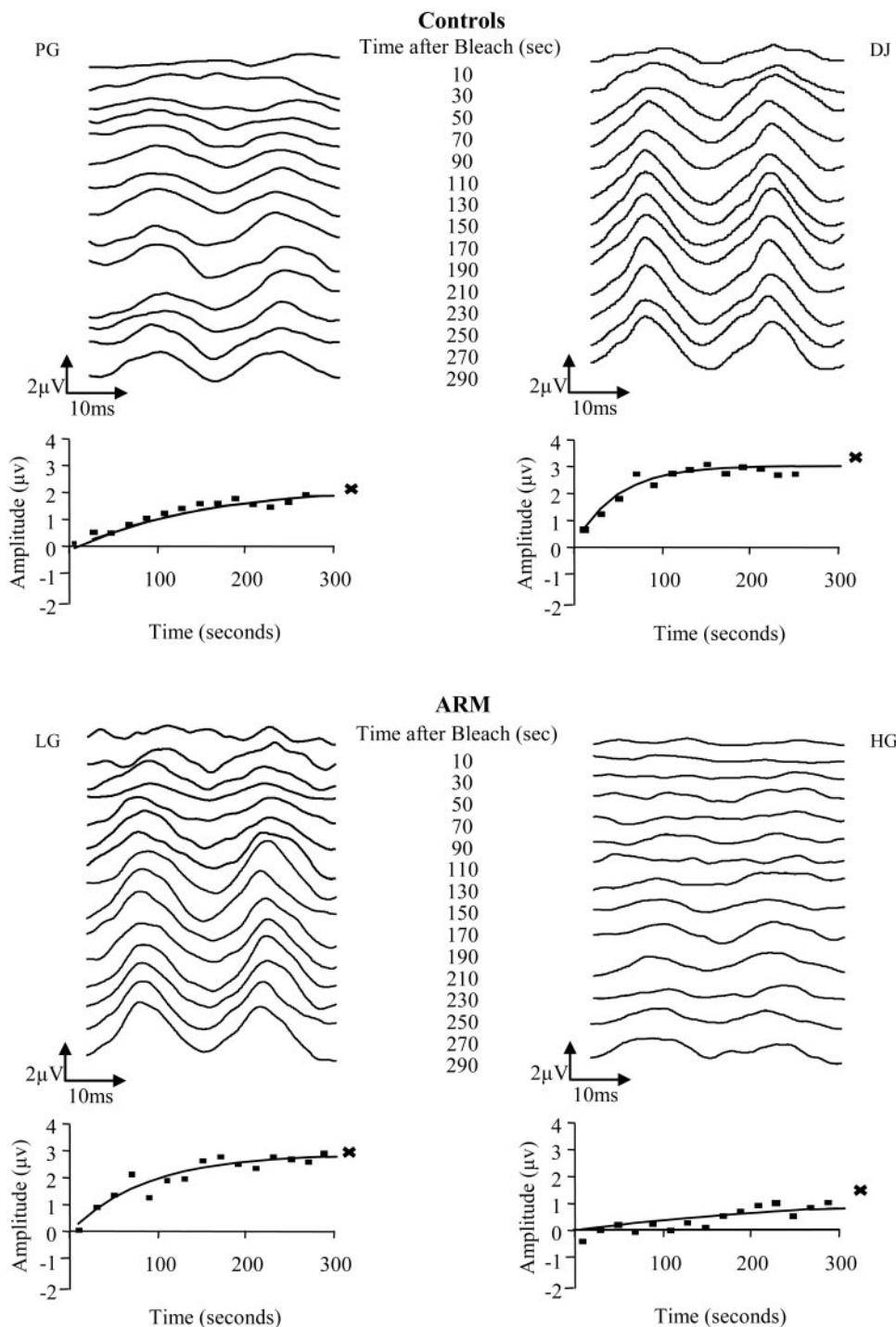
FIGURE 4. Typical ERG photostress test recovery data from two control subjects (*top traces*) and two participants with ARM (*bottom traces*). The ERG is markedly reduced in amplitude in all participants immediately after cessation of bleaching. Recovery of ERG amplitude followed an exponential time course. The X marker on each trace indicates the amplitude before bleaching.

this variability, focal-to-full-field amplitude ratios were calculated for each individual.

After Fourier analysis and removal of signals above 45 Hz, the mean amplitudes and implicit times of both the 5- and 41-Hz focal cone ERGs were obtained and are summarized in Table 2. The parameters that exhibited a statistically significant difference between the control and ARM groups were: the a- and b-wave implicit times of the transient response and the time-to-peak, peak-to-trough amplitude, and focal-to-full-field amplitude ratio of the first harmonic of the steady state response.

When individual ROC curves were constructed for these parameters, the transient focal cone ERG b-wave implicit time was marginally the best at discriminating participants with

ARM from the normal control subjects, yielding an area under the curve of 0.77. However, the transient focal cone ERG a-wave implicit time and the 41-Hz focal cone ERG amplitude, time-to-peak, and focal to full-field amplitude ratio all elicited a comparable area under the ROC curve (see Table 2).

To determine the extent to which the use of a focal to full-field amplitude ratio reduces between-participant variability, the coefficient of variation was calculated for both the amplitude and the ratio parameters. The parameter that was most affected by the calculation of an amplitude ratio was the 5-Hz focal cone ERG b-wave, which showed a marked reduction in the coefficient of variation, both in the control subjects (37%–23%) and in the participants with ARM (39%–33%). There was a smaller reduction in the coefficient of variation of
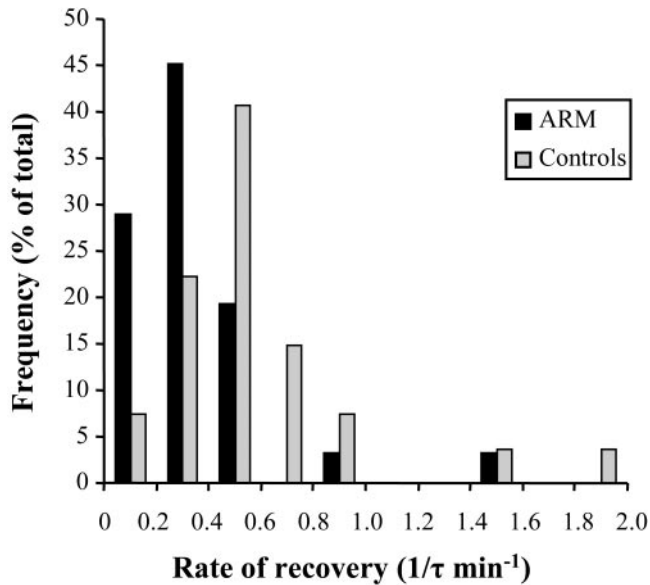
FIGURE 5. Histogram showing the distribution of rates of recovery of the ERG photostress test for control subjects and participants with ARM. Note that subjects with ARM tend to have a slower rate of recovery.

the 5-Hz a-wave amplitude when a ratio was calculated (control, 48%–45%; ARM, 45%–44%). The variability of the 41-Hz amplitude measures was reduced considerably in the ARM group (72%–57%), but was not improved in the control group (45%–46%). Nevertheless, the calculation of the amplitude ratio for the focal 41-Hz ERG still slightly improved the separation between groups (the area under the ROC curve changed from 0.73 to 0.74 with the calculation of the ratio).

Typical ERG photostress test responses from two control subjects and two participants with ARM are shown in Figure 4. The recovery data show that the ERG was virtually extinguished immediately after the bleaching, and gradually recovered over the following minutes. Participants with ARM tended to show a slower rate of recovery of ERG amplitude after light adaptation (Fig. 5). This was reflected in the significantly lower group-averaged rate of recovery in the ARM group compared to normal control subjects (Table 2). The large area under the ROC curve for this parameter (0.74) indicated that it provided good separation between the groups. Nine individuals with ARM and two control subjects had a particularly marked delay in recovery, failing to show any recovery within the 5-minute recording period. There was no significant correlation between visual acuity and rate of recovery in either the control (Spearman's rho = −0.11; *P* = 0.59) or ARM (Spearman's rho = −0.19; *P* = 0.30) group.

Logistic Regression Analysis

The univariate analysis identified six parameters that were significantly different between groups: the a- and b-wave im-

plicit times (5-Hz ERG); the implicit time, amplitude, and focal-to-full-field amplitude ratio (41-Hz ERG), and the rate of recovery of the ERG photostress test. These parameters were used as explanatory variables in the logistic regression analysis. The parameters of the best-fitting logistic regression model, shown in Table 3, were: the rate of recovery of the ERG photostress test, the b-wave implicit time of the 5-Hz focal cone ERG and the implicit time of the 41-Hz focal cone ERG. The area under the ROC curve was 0.84, indicating a good model fit, and, with a cutoff probability of *P* = 0.5, the sensitivity and specificity of the model were 77% and 85%, respectively.

DISCUSSION

In this study, that the recovery of the ERG photostress test was markedly slower in ARM and provides compelling evidence that the rate of recovery is an important electrophysiological predictor of ARM. In the univariate analysis, the rate of recovery of the ERG photostress test produced an impressive area under the ROC curve. Logistic regression analysis identified the ERG photostress test as an independent predictor of ARM. The logistic regression model enabled the exploitation of the full diagnostic potential of the entire test battery, providing an excellent area under the ROC curve and was able to distinguish between groups with a high sensitivity and specificity (77% and 85%, respectively).

The multivariate analysis identified three independent predictors of ARM, specifically: two latency measures and the ERG photostress test rate of recovery. This may reflect the presence of distinct pathogenic mechanisms.

A subset of nine individuals with ARM showed no recovery of ERG amplitude at all during the 5 minutes of recording after cessation of bleaching. Five of these participants had exudative AMD in the fellow eye. Given the known higher incidence of onset of choroidal neovascularization in the fellow eye of individuals with unilateral wet AMD,[40–42] this finding suggests that there is a slower rate of recovery in eyes with an increased risk of exudative changes. This result could indicate a prognostic role for the ERG photostress test in identifying, at an early stage, patients who may be suitable for future treatment interventions, such as photodynamic therapy.

The steady state 41-Hz ERG is largely dependent on bipolar cell activity.[31–34] However, the recovery of the 41-Hz ERG after exposure to intense light is primarily dependent on cone photopigment regeneration (although the nonlinear relation between photopigment recovery and voltage indicates that this relationship is a complex one).[30,43] This assertion is based on the fact that the recovery time constant obtained using the ERG photostress test is very similar to that for cone photopigment regeneration based on the measurement of photopic a-wave amplitudes.[30,43] Therefore, it is likely that the slower rate of recovery of the ERG photostress test reflects a deficit in the ability of the outer retina to regenerate cone photopigment. A delay in cone dark adaptation in ARM has been reported in the psychophysical literature,[44–47] however, the ERG photostress

TABLE 3. Parameters of the Best-Fitting Logistic Regression Model

Variable	Regression Coefficient ± SEM	Significance	Odds Ratio (95% CI)
Rate of recovery (1/τ min⁻¹)	−2.44 ± 1.16	0.04	0.09 (0.013–0.591)
Focal b-wave implicit time (ms)	0.49 ± 0.18	0.007	1.64 (1.22–2.21)
Focal 41-Hz implicit time (ms)	0.43 ± 0.23	0.07	1.53 (1.04–2.25)
Constant	−26.08 ± 7.94	0.001	

Three parameters were identified as contributing to the best-fitting model, which yielded a sensitivity and specificity of 77% and 85%, respectively, at distinguishing between ARM and normal control groups. The area under the ROC curve was 0.84.

test provides a unique means of objectively assessing this impairment at an outer retinal level.

Retinal adaptation is a complex process that requires the provision of retinoids and metabolites by the choroidal blood supply. These materials must be transported across Bruch's membrane to the RPE and photoreceptors where the regeneration of photopigment occurs.[48] Structural changes to Bruch's membrane, such as thickening and the accumulation of hydrophobic materials,[49] and atrophy of the choriocapillaris[50] may limit the rate at which these essential molecules reach the outer retina in ARM, thus causing slowed adaptation kinetics.[23,51] The alteration to the permeability of Bruch's membrane in ARM not only affects the rate of photopigment regeneration, but has also been linked to the onset of choroidal neovascularization, through the disruption of the transport of RPE-derived growth factors to the choriocapillaris via Bruch's membrane.[52] This common causal factor may explain the link between slower cone dark adaptation and an increased risk of exudative AMD.

Participants in this study were classified as normal or having ARM on the basis of fundus appearance and visual acuity, alone. It is noteworthy that two participants within the control group showed no recovery in the 5-minute recording period. This suggests that the ERG photostress test highlights functional abnormalities that are not reflected in the fundus appearance. Longitudinal evaluation would determine whether the electrophysiological tests are detecting participants within the control group who are at a subclinical stage of ARM.

Abnormal adaptation kinetics have been reported in other macular conditions, such as Sorsby's fundus dystrophy,[53–56] idiopathic central serous chorioretinopathy,[57,58] Stargardt's disease, and fundus flavimaculatus (Marinescu AIC et al. *IOVS* 2001;42:ARVO Abstract 351).[59–62] It is important, therefore, that the full clinical profile of the patient be considered if the ERG photostress test is to be used diagnostically. For example, the discrepancy in the usual age of onset of these other macular conditions (typically before the fifth decade of life) and ARM (typically in the sixth decade or above) should be taken into account in the differential diagnosis. Further investigation using the ERG photostress test will determine the potential for the assessment of patients with macular conditions other than ARM.

To conclude, the ERG photostress test rate of recovery was found to be significantly reduced in subjects with ARM and was a significant predictor of ARM in the best-fitting logistic regression model. Improved assessment of the functional integrity of the central retina will facilitate both evaluation of therapeutic interventions and earlier identification of those with a heightened risk of ARM.

References

1. Klein R, Klein BE, Cruickshanks KJ. The prevalence of age-related maculopathy by geographic region and ethnicity. *Prog Retin Eye Res*. 1999;18:371–389.
2. Wang JJ, Foran S, Mitchell P. Age-specific prevalence and causes of bilateral and unilateral visual impairment in older Australians: the Blue Mountains Eye Study. *Clin Exp Ophthalmol*. 2000;28:268–273.
3. Bird AC, Bressler NM, Bressler SB, et al. An international classification and grading system for age-related maculopathy and age-related macular degeneration. The International ARM Epidemiological Study Group. *Surv Ophthalmol*. 1995;39:367–374.
4. Criswell MH, Ciulla TA, Lowseth LA, Small W, Danis RP, Carson DL. Anastomotic vessels remain viable after photodynamic therapy in primate models of choroidal neovascularization. *Invest Ophthalmol Vis Sci*. 2005;46:2168–2174.
5. Weber U, Hecker H. Transpupillary thermotherapy for occult choroidal neovascularizations. *Ophthalmologe*. 2005;102:355–362.
6. Jaakkola A, Heikkonen J, Tommila P, Laatikainen L, Immonen I. Strontium plaque brachytherapy for exudative age-related macular degeneration: three-year results of a randomized study. *Ophthalmology*. 2005;112:567–573.
7. Michels S, Rosenfeld PJ. Treatment of neovascular age-related macular degeneration with Ranibizumab/Lucentis(TM). *Klin Monatsbl Augenheilkd*. 2005;222:480–484.
8. Pawlak D, Glacet-Bernard A, Papp M, Coscas G, Soubrane G. Results of limited macular translocation in subfoveal choroidal neovascularization in age-related macular degeneration. *J Fr Ophtalmol*. 2004;27:3S31–3S37.
9. Falsini B, Fadda A, Iarossi G, et al. Retinal sensitivity to flicker modulation: reduced by early age-related maculopathy. *Invest Ophthalmol Vis Sci*. 2000;41:1498–1506.
10. Birch DG, Fish GE. Focal cone electroretinograms: aging and macular disease. *Doc Ophthalmol*. 1988;69:211–220.
11. Sandberg MA, Miller S, Gaudio AR. Foveal cone ERGs in fellow eyes of patients with unilateral neovascular age-related macular degeneration. *Invest Ophthalmol Vis Sci*. 1993;34:3477–3480.
12. Sandberg MA, Weiner A, Miller S, Gaudio AR. High-risk characteristics of fellow eyes of patients with unilateral neovascular age-related macular degeneration. *Ophthalmology*. 1998;105:441–447.
13. Remulla JF, Gaudio AR, Miller S, Sandberg MA. Foveal electroretinograms and choroidal perfusion characteristics in fellow eyes of patients with unilateral neovascular age-related macular degeneration. *Br J Ophthalmol*. 1995;79:558–561.
14. Li J, Tso MO, Lam TT. Reduced amplitude and delayed latency in foveal response of multifocal electroretinogram in early age related macular degeneration. *Br J Ophthalmol*. 2001;85:287–290.
15. Gerth C, Hauser D, Delahunt PB, Morse LS, Werner JS. Assessment of multifocal electroretinogram abnormalities and their relation to morphologic characteristics in patients with large drusen. *Arch Ophthalmol*. 2003;121:1404–1414.
16. Heinemann-Vernaleken B, Palmowski AM, Allgayer R, Ruprecht KW. Comparison of different high resolution multifocal electroretinogram recordings in patients with age-related maculopathy. *Graefes Arch Clin Exp Ophthalmol*. 2001;239:556–561.
17. Curcio CA. Photoreceptor topography in ageing and age-related maculopathy. *Eye*. 2001;15:376–383.
18. Curcio CA, Medeiros NE, Millican CL. Photoreceptor loss in age-related macular degeneration. *Invest Ophthalmol Vis Sci*. 1996;37:1236–1249.
19. Owsley C, Jackson GR, Cideciyan AV, et al. Psychophysical evidence for rod vulnerability in age-related macular degeneration. *Invest Ophthalmol Vis Sci*. 2000;41:267–273.
20. Brown B, Tobin C, Roche N, Wolanowski A. Cone adaptation in age-related maculopathy. *Am J Optom Physiol Opt*. 1986;63:450–454.
21. Feigl B, Brown B, Lovie-Kitchin J, Swann P. Cone- and rod-mediated multifocal electroretinogram in early age-related maculopathy. *Eye*. 2005;19:431–441.
22. Chen C, Wu L, Wu D, et al. The local cone and rod system function in early age-related macular degeneration. *Doc Ophthalmol*. 2004;109:1–8.
23. Owsley C, Jackson GR, White M, Feist R, Edwards D. Delays in rod-mediated dark adaptation in early age-related maculopathy. *Ophthalmology*. 2001;108:1196–1202.
24. Phipps JA, Guymer RH, Vingrys AJ. Loss of cone function in age-related maculopathy. *Invest Ophthalmol Vis Sci*. 2003;44:2277–2283.
25. Sunness JS, Massof RW, Johnson MA, Finkelstein D, Fine SL. Peripheral retinal function in age-related macular degeneration. *Arch Ophthalmol*. 1985;103:811–816.
26. Jackson GR, McGwin G Jr, Phillips JM, Klein R, Owsley C. Impact of aging and age-related maculopathy on activation of the a-wave of the rod-mediated electroretinogram. *Invest Ophthalmol Vis Sci*. 2004;45:3271–3278.
27. Sandberg MA, Pawlyk BS, Berson EL. Isolation of focal rod electroretinograms from the dark-adapted human eye. *Invest Ophthalmol Vis Sci*. 1996;37:930–934.
28. Lovasik JV. An electrophysiological investigation of the macular photostress test. *Invest Ophthalmol Vis Sci*. 1983;24:437–441.
29. Parisi V. Electrophysiological evaluation of the macular cone adaptation: VEP after photostress: a review. *Doc Ophthalmol*. 2001;102:251–262.

30. Binns AM, Margrain TH. Evaluation of retinal function using the dynamic focal cone ERG. *Ophthalmic Physiol Opt*. 2005;25:492–500.

31. Kondo M, Sieving PA. Post-photoreceptoral activity dominates primate photopic 32-Hz ERG for sine-, square-, and pulsed stimuli. *Invest Ophthalmol Vis Sci*. 2002;43:2500–2507.

32. Kondo M, Sieving PA. Primate photopic sine-wave flicker ERG: vector modeling analysis of component origins using glutamate analogs. *Invest Ophthalmol Vis Sci*. 2001;42:305–312.

33. Hare WA, Ton H. Effects of APB, PDA, and TTX on ERG responses recorded using both multifocal and conventional methods in monkey: effects of APB, PDA, and TTX on monkey ERG responses. *Doc Ophthalmol*. 2002;105:189–222.

34. Viswanathan S, Frishman LJ, Robson JG. Inner-retinal contributions to the photopic sinusoidal flicker electroretinogram of macaques: macaque photopic sinusoidal flicker ERG. *Doc Ophthalmol*. 2002;105:223–242.

35. Dawson WW, Trick GL, Litzkow CA. Improved electrode for electroretinography. *Invest Ophthalmol Vis Sci*. 1979;18:988–991.

36. Wyszeki G, Stiles WS. *Colour Science: Concepts and Methods, Quantitative Data and Formulae*. New York: John Wiley; 1982.

37. Aguilar M, Stiles WS. Saturation of the rod mechanism of the retina at high levels of stimulation. *Opt Acta*. 1954;1:59–65.

38. Sharpe LT, Stockman A. Rod pathways: the importance of seeing nothing. *Trends Neurosci*. 1999;22:497–504.

39. Hollins M, Alpern M. Dark adaptation and visual pigment regeneration in human cones. *J Gen Physiol*. 1973;62:430–447.

40. Strahlman ER, Fine SL, Hillis A. The second eye of patients with senile macular degeneration. *Arch Ophthalmol*. 1983;101:1191–1193.

41. Roy M, Kaiser-Kupfer M. Second eye involvement in age-related macular degeneration: a four-year prospective study. *Eye*. 1990;4:813–818.

42. Klein R, Klein BE, Jensen SC, Meuer SM. The five-year incidence and progression of age-related maculopathy: the Beaver Dam Eye Study. *Ophthalmology*. 1997;104:7–21.

43. Mahroo OA, Lamb TD. Recovery of the human photopic electroretinogram after bleaching exposures: estimation of pigment regeneration kinetics. *J Physiol*. 2004;554:417–437.

44. Wu G, Weiter JJ, Santos S, Ginsburg L, Villalobos R. The macular photostress test in diabetic retinopathy and age-related macular degeneration. *Arch Ophthalmol*. 1990;108:1556–1558.

45. Cheng AS, Vingrys AJ. Visual losses in early age-related maculopathy. *Optom Vis Sci*. 1993;70:89–96.

46. Sandberg MA, Gaudio AR. Slow photostress recovery and disease severity in age-related macular degeneration. *Retina*. 1995;15:407–412.

47. Midena E, Angeli CD, Blarzino MC, Valenti M, Segato T. Macular function impairment in eyes with early age-related macular degeneration. *Invest Ophthalmol Vis Sci*. 1997;38:469–477.

48. Saari JC. Biochemistry of visual pigment regeneration: the Friedenwald lecture. *Invest Ophthalmol Vis Sci*. 2000;41:337–348.

49. Starita C, Hussain AA, Pagliarini S, Marshall J. Hydrodynamics of ageing Bruch's membrane: implications for macular disease. *Exp Eye Res*. 1996;62:565–572.

50. Friedman E, Krupsky S, Lane AM, et al. Ocular blood flow velocity in age-related macular degeneration. *Ophthalmology*. 1995;102:640–646.

51. Marshall J, Hussain AA, Starita C, Moore DJ, Patmore AL. Aging and Bruch's membrane. In: Marmor MF, Wolfensberger TJ, eds. *The Retinal Pigment Epithelium: Function and Disease*. New York: Oxford University Press; 1998:669–692.

52. Moore DJ, Hussain AA, Marshall J. Age-related variation in the hydraulic conductivity of Bruch's membrane. *Invest Ophthalmol Vis Sci*. 1995;36:1290–1297.

53. Cideciyan AV, Pugh EN, Lamb TD, Huang YJ, Jacobson SG. Plateaux during dark adaptation in Sorsby's fundus dystrophy and vitamin A deficiency. *Invest Ophthalmol Vis Sci*. 1997;38:1786–1794.

54. Jacobson SG, Cideciyan AV, Regunath G, et al. Night blindness in Sorsbys-fundus-Dystrophy reversed by vitamin-A. *Nat Genet*. 1995;11:27–32.

55. Lip PL, Good PA, Gibson JM. Sorsby's fundus dystrophy: a case report of 24 years follow-up with electrodiagnostic tests and indocyanine green angiography. *Eye*. 1999;13:16–25.

56. Steinmetz RL, Polkinghorne PC, Fitzke FW, Kemp CM, Bird AC. Abnormal dark-adaptation and rhodopsin kinetics in Sorsby's fundus dystrophy. *Invest Ophthalmol Vis Sci*. 1992;33:1633–1636.

57. Wang M, Sander B, Lund-Andersen H, Larsen M. Detection of shallow detachments in central serous chorioretinopathy. *Acta Ophthalmol Scand*. 1999;77:402–405.

58. Horiguchi M, Ito Y, Miyake Y. Extrafoveal photostress recovery test in glaucoma and idiopathic central serous chorioretinopathy. *Br J Ophthalmol*. 1998;82:1007–1012.

59. Derwent JJK, Derlacki DJ, Hetling JR, et al. Dark adaptation of rod photoreceptors in normal subjects, and in patients with Stargardt disease and an ABCA4 mutation. *Invest Ophthalmol Vis Sci*. 2004;45:2447–2456.

60. Fishman GA, Farbman JS, Alexander KR. Delayed rod dark-adaptation in patients with Stargardt disease. *Ophthalmology*. 1991;98:957–962.

61. Itabashi R, Katsumi O, Mehta MC, Wajima R, Tamai M, Hirose T. Stargardt disease fundus flavimaculatus: psychophysical and electrophysiologic results. *Graefes Arch Clin Exp Ophthalmol*. 1993;231:555–562.

62. Parisi V, Canu D, Iarossi G, Olzi D, Falsini B. Altered recovery of macular function after bleaching in Stargardt's disease-fundus flavimaculatus: pattern VEP evidence. *Invest Ophthalmol Vis Sci*. 2002;43:2741–2748.